ELSEVIER

Chemical Engineering Journal 70 (1998) 143–155

Chemical Engineering Journal

On the lower operating range of sieve and valve trays

E.F. Wijn [1]*

Meteorenweg 1014, 1443 BD Purmerend, Netherlands

Received 19 November 1997; accepted 18 March 1998

Abstract

A model of the lower operating limits of distillation and absorption trays is described in this paper. The model requires the simultaneous solution of two equations describing (1) liquid flow across the tray and over the outlet weir, and (2) countercurrent liquid flow through the free hole area of the tray. The second equation stems from models of a tray without downcomers; this equation was validated by means of available test data. The model gives liquid height and weep fraction as a function of gas and liquid flow rates, for a given tray layout. As shown, it permits calculation of the gas flow rate at weep and seal point, in a coherent way. Examples illustrate the use of the method in calculating the position of the weeping range of a tray and its relation to tray efficiency.

Keywords: Absorption; Distillation; Dumping; Seal point; Sieve tray; Valve tray; Weeping; Weep point

1. Introduction

Trays in absorption or distillation columns only work well over a limited range of vapour and liquid loadings. Both the design engineer and the column operator need to know the upper and lower operating limits. Current process simulation programmes have a limited capability to describe the turndown characteristics of trayed columns. This topic was identified as needing further development, for use in rate based models in process simulating software [1].

Sieve trays came in widespread use, in the 1950–1960 period. Distillation columns provided with sieve trays were shown to enable much higher column throughputs than columns with bubble cap trays, which had been in use before. Contrary to bubble cap trays, sieve trays have a lower operating limit. During the sieve tray introduction phase, some research was devoted to this topic. The lower operating limit was shown to be due to leakage of liquid through the perforations in the tray upon lowering the vapour flow rate. Some years later, efforts to develop trays combining a high capacity with an enlarged operating range resulted in the introduction of several types of valve trays. A valve tray is a sieve tray with large holes, with a disc mounted over each hole which is movable only within set limits. At a sufficiently high vapour flow rate the discs (valves) are lifted by the vapour flow and the holes are opened. Lowering the vapour flow eventually let the discs fall back on the tray, closing off the holes and stopping the leakage of liquid.

It has traditionally been assumed that the gas rate below which liquid starts to leak through the perforations (i.e., the weep point) is the lower operating limit. For many applications, this is known to be conservative. A tray can have a good separation performance far below the weep point [2–4], as long as there is sufficient liquid hold up on the tray to allow for mass transfer. A more appropriate lower limit is the seal point [5], i.e., the gas rate below which the full liquid flow leaks away through the perforations and no liquid flows anymore over the outlet weir and through the downcomer. In the weeping range between weep and seal point, the liquid flow pattern switches from cross flow on the tray to countercurrent gas–liquid flow through the perforations.

For conventional sieve and valve trays, the upper operating limits are well documented. The lower operating limits are less well-established and predictable. This paper describes a hydrodynamic model of the whole lower operating range of trays. It allows calculation of the weep point, the seal point and also the weep fraction.

2. Tray operation

2.1. General hydrodynamic behaviour

During normal operation of a tray, the flow regime of the two phase dispersion in the contacting area is usually either

* Corresponding author. Internet: http://www.euronet.nl/~wijnef.

[1] Formerly: Shell Research, Amsterdam, The Netherlands.

1385-8947/98/$19.00
PII S1385-8947(98)00089-8

in the *spray*- or in the (*mixed*) *froth* regime (which is also identified as the *churn turbulent* regime or the *heterogeneous bubbling* regime). In the spray regime, the gas phase is the continuous phase and the liquid phase is being atomised. Droplets move around on random ballistic trajectories in the intertray space. The droplet population has a wide size and velocity distribution. Operation in the spray regime is associated with low liquid rates, low liquid hold ups and high gas rates. Conversely, operation in the heterogeneous bubbling regime is favoured by high liquid rates, high liquid hold ups and low gas rates. In this regime, the two phase layer consists of two layers, at least. These two layers are a dense bottom layer and a low density spray top layer, with a transition from a liquid-continuous phase to a gas-continuous phase taking place in between. A fairly gas free liquid layer is located directly above the perforations. The top layer always consists of a low density spray layer, in which droplets move in a random ballistic way in a continuous gas phase. The contribution of this spray layer to the dispersion height varies considerably, depending on operating conditions, system properties, tray type and geometry.

When a tray is operated near its lower limits, it will usually be in the heterogeneous bubbling regime. The tray then contains a two phase dispersion with a liquid volume fraction, ε_l varying between 0.4 to 0.8. The dispersion is much denser than when the trays operate near its upper limit ($\varepsilon_l \cong 0.1$ to 0.2). The heterogeneous bubbling bed has a highly dynamic character. There are continuously fluctuations in the bed height, bed density and pressure drop. The rise time for the bubbles is long enough for bubble coalescence and break up processes to take place. Coalescence depends, among others, on bubble concentration, bubble size and surface properties. Break up depends on bubble size, surface tension and the random movements in the dispersion, caused by the kinetic energy imparted by the passing gas. Together, the break up and coalescence processes lead to a dynamic equilibrium of the bubble size and the bubble rise velocity distributions. The random liquid movement also feeds back into the bubble formation process itself, causing desynchronisation of bubble formation at adjacent holes, randomisation of the bubble formation period and stimulation of the occurrence of weepage. Because the flow on a tray is so complicated, most of the current descriptions are purely empirical. We can only describe what is going on in terms of 'averaged properties'.

2.2. Characteristics of the lower range of operation

Upon lowering the gas flow rate through a tray a point is reached below which the separation performance starts to decline. From visual observations of the tray behaviour in test stands, it has become apparent that two different 'critical' gas flowrates can be identified. When lowering the gas rate, first the weep point is reached, at which liquid starts to leak through the perforations and the perforations are no longer used exclusively for gas passage. Further lowering the gas rate results in an increasing weep rate and lowering of the dispersion height. Ultimately, the gas rate becomes so low that the dispersion is not expanded sufficiently to let any liquid flow over the outlet weir into the downcomer. Liquid no longer being supplied from the tray above, a liquid level in the downcomer cannot be maintained and the downcomer outlet may loose its sealing; the seal point has been reached. In the literature, this point has also been called the dump point.

Three different conditions can be recognised in the lower range of operation: (1) At rates below the *seal point* (the dumping range), both gas and liquid flow through the perforated area of the tray and no liquid flows through the downcomer. The hydraulic behaviour has become equivalent to that of a tray without downcomers; a dual flow tray. (2) *Between weep point and seal point* (the weeping range), the liquid flow switches from flow across the tray to a condition of countercurrent flow through the perforations. (3) At gas rates in excess of the *weep point* (the normal operating range), the perforations are utilised by the gas flow exclusively. The entire liquid flow rate is transported over the outlet weir and through the downcomer.

This picture may be augmented by one or more of the following phenomena.

- *Blowing* occurs when (part of) the gas flows up through the downcomer with a high velocity. Part of any liquid flow going into the downcomer may be blown up and out of the downcomer again. This mode of operation directly affects the weep rate, because the gas flow rate through the perforated area is reduced significantly. Moreover, because the gas flowing through the downcomer bypasses the contacting area, a significant loss in mass transfer performance occurs. Blowing develops when the exit of the downcomer is no longer submerged in the dispersion on the tray below. At operation below the seal point, this is normally the case. However, it can also develop at gas rates far above the seal point, whenever the static liquid head building up in the downcomer is insufficient to counterbalance the pressure drop of the tray, as for instance during column start up periods. When it develops under these circumstances, the gas blowing action can be quite violent and may result in a maloperation of a tray (or trays). A good tray design prevents this from happening.
- *Oscillations* and *pulsations* are macro scale fluctuations, which introduce a degree of order and structure in the otherwise highly dynamic and disordered two phase layer. Oscillations are wave like fluctuations in dispersion height, sloshing from side-to-side. The downstroke of such a wave enhances weeping, while the upstroke increases entrainment, see among others: Refs. [6–8]. Oscillations usually occur at gas flow rates, which are roughly twice as high as the rate needed to stop weeping. Pulsations are vertical up and down movements of the dispersion as a whole, caused by synchronised periodic injection of gas through all the perforations. These pulsations are driven by a large, cyclic variation of the pressure in the gas space underneath the tray, see Wijn [9]. Pulsations increase both the weep rate and the entrainment rate in comparison to non-pulsating conditions. Pulsations

tend to occur mainly in the lower operating range of a tray, around the seal point.

- *A hydraulic gradient* in the direction of liquid flow may lead to longitudinal maldistribution of vapour flowing through the contacting area. This can be detrimental to the separation performance of the tray by causing vapour cross flow channelling, see Kister et al. [10]. Hydraulic gradients may be caused by a hydraulic jump directly downstream of a downcomer exit (at the inlet of a tray), the resistance to flow of liquid across a tray and by weeping on a tray with a long flow path in combination with a large free hole area.
- *Non-uniform flow patterns* may develop because of tilt or sag of a tray. Under normal operating conditions, this leads to maldistributed flows of gas and liquid and a loss in the separation performance of the tray. Clear liquid zones (with liquid flow, but no gas flow) or stagnant zones (with gas flow, but no liquid flow) are easily recognisable manifestations of these flow patterns. Eventually, the two phase layer may degenerate into a 'froth bed collapse' (see Lockett [11]) with even more severe consequences for the mass transfer on the tray. Operation in the lower range of a tray may also lead to the development of non-uniformity, as will be indicated later.

Another cause of non-uniformity is the presence of bounding walls, baffles and weirs. These cause liquid circulation cells by a difference in density between the dispersion near these walls and further away. This 'wall effect' is already present in the normal operating range and extends into the weeping and dumping ranges. The static pressure difference and the associated liquid movement preferentially cause weeping near these walls.

Still another non-uniform flow pattern exists, which is characteristic of operation in the heterogeneous bubbling regime. This is the presence of stationary or moving liquid circulation patterns in the two phase layer, see Beek [12] and Haug [13]. These circulation patterns can get organised into a large scale maldistribution of the gas- and liquid flows, which can cause non-uniform weeping patterns.

With all this in mind, a model has been set up to describe the behaviour of a tray between the weep point and the seal point. This model describes the switching over from the normal cross flow of liquid on the tray to the countercurrent flow of liquid through the tray. It builds on previous work done by Lockett and Banik [14] and Banik [15]. Also it provides a link with the earlier study of Prince and Chan [5], describing the seal point.

2.3. The two region approach

The two phase layer is assumed to be a heterogeneous bubbling dispersion. If we were to take pictures of the bubble formation process at a hole, we would see an irregular process due to random motions of the surrounding dispersion. A bubble forms by gas flowing upward through the hole. It than breaks away and liquid can flow through the hole until the next bubble starts to form. So, there are two parts in the cycle: one with gas flowing through the holes and one with liquid flowing. At each moment a certain fraction of the holes will carry the gas flow and the rest will carry the liquid flow. The model needs the average fractions of the two kinds of holes.

The bubble formation process has been studied by Prado [16] and many others. Moreover, Prado confirmed (by his measurements of the liquid bridging frequency) that the two stage bubble formation model of Wraith [17] describes the random formation period on his sieve trays. This enabled him to use Wraith's model for calculating the bubble size at formation.

During the gassing part of the bubble formation cycle, the rate of inflow of gas into the forming bubble is time dependent. This results in a time-dependent gas pressure drop across the hole. The time averaged value for the pressure drop with a varying gas flow rate is larger than for a steady gas flow, with the same time averaged volumetric flow rate. This is caused by the nonlinear (quadratic) dependency of the pressure drop on gas flow rate. Assuming that the wave shape of flow rate (and hence the relative pressure drop) fluctuations remain constant, the flow resistance coefficient will be enlarged by a constant factor. By analogy, this holds for the leaking liquid, as well.

When during the operation of a tray the flow regime changes from the bubbling regime to the jetting regime, the operative mechanism at the holes changes as well. The transition from an unsteady, bubbling process to a steady, jetting process greatly influences the hydrodynamic behaviour and the model will later have to be adapted to take this into account. So, the transition from the heterogeneous bubbling (or mixed froth) regime to the spray will limit the range of applicability of the present approach.

3. Modelling the lower operating range

The next paragraphs discuss the dumping range, weeping range and normal operating range of a tray. The diagrams given in Fig. 1 may be helpful in following this sequence and the more detailed arguments being given below.

The following treatment makes use of two equations for the liquid height on a tray. The first is a classical equation, which sums a weir height contribution and the Francis' weir flow contribution. The second equation considers flow through the tray such as occurs on a tray without downcomers (a 'dual flow' tray). This second equation is not commonly used, although it has its predecessors. An example is the description of the tray pressure drop at the seal point by Prince and Chan [5]. The new liquid height model is based on averaging overall pressure drop balances.

Combining a linearized version of the H_L-relation for the dumping range operation with a linearized version of the H_L-relation for the normal operating range gives explicit relations for the weep fraction, weep point and seal point. These equations will be validated later on.

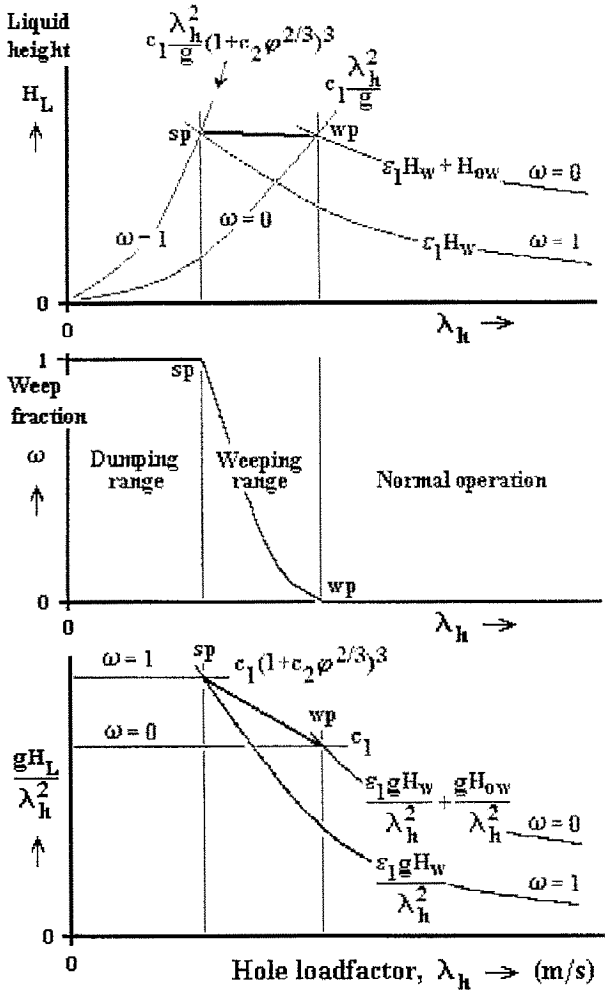

Fig. 1. Overview of principles.

3.1. Dumping range

Upon operation at gas flow rates below the seal point, all liquid flow is leaking ($\omega = 1$) and all gas is assumed to be flowing through the contacting area (no bypassing). The flow conditions are analogous to that on a tray without downcomers (a 'dual flow' tray).

A time-invariant model can be set up, in which the contacting area of the tray is considered to be subdivided in two zones, see Fig. 2. One zone consists of the area made up by the bubbling holes, through which the gas flows (the 'gassing' zone). The other zone consists of the holes leaking liquid (the 'leaking' zone).

The model does not take time variations of the gas flow rate (and pressure drop) into account, even so, it appears to contain much of the time averaged behaviour of a tray. For reasons of simplicity, the possibility that part of the holes (and the contacting area) is stagnant (not actively contributing to either gas flow or liquid flow) has been omitted. This complication could be included later also, if deemed necessary.

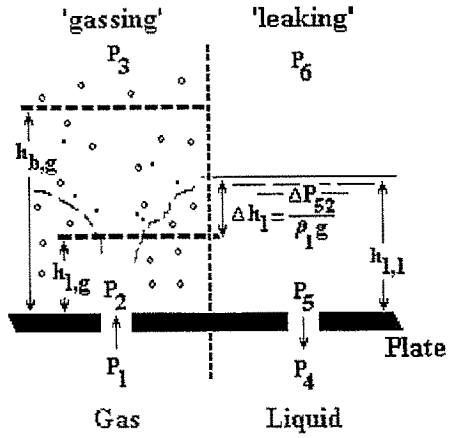

Fig. 2. Conceptual subdivision.

3.1.1. Basic pressure drop relations

The fraction of holes (and also the fraction of bubbling area) carrying the gas flow is defined as f_g. The fraction of holes (and fraction of bubbling area) contributing to leakage, will be $f_l (= 1 - f_g)$.

The pressure drop for gas flowing through the holes in the 'gassing' zone in the plate can be written as (Fig. 3):

$$P_1 = P_2 + \frac{\xi_g \rho_g V_{gh}^2}{2 f_g^2} \qquad (3.1.1.1)$$

ξ_g is the resistance coefficient for the gas flow. Note that V_{gh} is based on *total* hole area.

For the liquid flowing through the holes in the 'leaking' zone, one can write:

$$P_4 = P_5 + \frac{\xi_l \rho_l V_{lh}^2}{2 f_l^2} \qquad (3.1.1.2)$$

Here it should be noted that V_{lh} is based on the definition, that *all* liquid fed to the tray flows through the *total* hole area as *clear* (non-aerated) liquid. ξ_l is the resistance coefficient for this flow through the holes.

As pressures P_1 and P_4 are the same and equal, the pressure difference between the 'gassing' zone and the 'leaking' zone is:

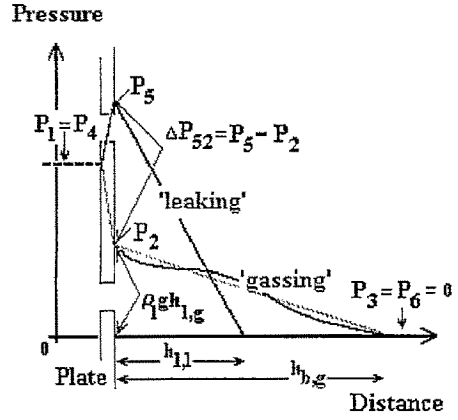

Fig. 3. Pressure drop vs. vertical distance.

$$P_5-P_2=\frac{\xi_g\rho_g V_{gh}^2}{2f_g^2}+\frac{\xi_l\rho_l V_{lh}^2}{2(1-f_g)^2} \quad (3.1.1.3)$$

Inspection of this relationship reveals that (P_5-P_2) goes through a minimum upon varying f_g. The pressure drop (P_5-P_2) constitutes a driving force for horizontal liquid flow across the plate from the 'leaking' zone to the 'gassing' zone of the tray. In this context, it is assumed that the system will settle at the minimum value for the pressure difference (P_5-P_2). Operation away from this minimum would cause pressure differentials to develop, which would drive the system back to its minimum. Fluctuations shown by the heterogeneous bubbling system help to keep it moving around this minimum in pressure drop, on a time averaged basis.

With (P_5-P_2) being at its minimum value, the liquid flow from the 'leaking' zone to the 'gassing' zone will be at its minimum. This liquid flow is pumped to a higher potential energy-level in the 'gassing' zone of the tray and will recycle from there to the 'leaking' zone. Minimisation of the driving force for this recirculating liquid flow minimises the liquid flow rate itself. This leads also to the minimisation of the power that needs to be expended in keeping this flow going. Hence, in effect, the minimum energy dissipation principle has been invoked.

Differentiating the above relation with respect to f_g leads to $d(P_5-P_2)/df_g=0$:

$$P_5-P_2=\left(\sqrt[3]{\frac{\xi_g\rho_g V_{gh}^2}{2}}+\sqrt[3]{\frac{\xi_l\rho_l V_{lh}^2}{2}}\right) \quad (3.1.1.4)$$

$$\text{and } f_g=\frac{1}{1+\sqrt[3]{\frac{\xi_l\rho_l V_{lh}^2}{\xi_g\rho_g V_{gh}^2}}}$$

Introducing the flow parameter based on hole area, defined as $\varphi_h=V_{lh}/V_{gh}\sqrt{\rho_l/\rho_g}$, then gives the pressure difference as:

$$\Delta P_{52}=P_5-P_2=\frac{\xi_g\rho_g V_{gh}^2}{2}\left\{1+\sqrt[3]{\frac{\xi_l\varphi_h^2}{\xi_g}}\right\}^3 \quad (3.1.1.5)$$

$$\text{and } f_g=\frac{1}{1+\sqrt[3]{\frac{\xi_l\varphi_h^2}{\xi_g}}}$$

3.1.2. Average liquid height on a dumping tray

This section explores a description of the hydraulics of a weeping tray. This will be done by developing a liquid height relation based on the assumption that the hydrostatic head of liquid, $h_{l,g}$, will be proportional to the gas velocity head in the holes. When the liquid height is larger, the hydrostatic head will stop the gas flow and the holes will revert to leaking.

In general, the average clear (non-aerated) liquid height on the total bubbling area will be given by:

$$H_L=f_g h_{l,g}+(1-f_g)h_{l,l} \quad (3.1.2.1)$$

also, equally general:

$$h_{l,l}=h_{l,g}+\frac{(P_5-P_2)}{\rho_l g} \quad (3.1.2.2)$$

A relationship describing $h_{l,g}$ will be needed to proceed any further. The following *assumed* relationship for the liquid head (which can be tolerated without leakage) was used:

$$\rho_l g h_{l,g}=\frac{\xi_{g,g}\rho_g V_{gh}^2}{2f_g^2} \quad (3.1.2.3)$$

Substituting this relation in the above given general equations, also using the relations for f_g and (P_5-P_2), first we find:

$$H_L=h_{l,g}+(1-f_g)\frac{(P_5-P_2)}{\rho_l g} \quad (3.1.2.4)$$

and subsequently:

$$gH_L=\frac{\xi_g\lambda_h^2}{2}\left(\frac{\xi_{g,g}}{\xi_g}+\sqrt[3]{\frac{\xi_l\varphi_h^2}{\xi_g}}\right)\left(1+\sqrt[3]{\frac{\xi_l\varphi_h^2}{\xi_g}}\right)^2 \quad (3.1.2.5)$$

As long as the gas flow resistance coefficients are similar, $\xi_{g,g}/\xi_g\cong 1$, the above relation reduces to the non-dimensional equation:

$$gH_L=c_1\lambda_h^2(1+c_2\sqrt[3]{\varphi^2})^3 \quad (3.1.2.6)$$

or in dimensional form:

$$H_L=\frac{c_1\lambda_h^2}{g}(1+c_2\sqrt[3]{\varphi^2})^3. \quad (3.1.2.7)$$

The dimensionless relation can conveniently be used to bring order in the available experimental data. The values for the coefficients c_1, c_2 are expected to be specific for different types of trays and will depend on hole shape and geometry. A non-steady gas flow will alter coefficient c_1, because of large variations in gas flow rate and hole pressure drop related to the bubbling process. In case of aeration of the clear liquid phase with small bubbles having a low rise velocity, the result will be a liquid phase carrying a gas fraction, $\varepsilon_{g,em}$ and having an 'emulsified' appearance. Its primary influence will be on coefficient c_2, which will depend on $c_2\propto 1/(1-\varepsilon_{g,em})$, as a result of the increased volumetric flow of the aerated liquid phase and its reduced density.

In itself, the model developed above does not exclude large scale non-uniformity of the distribution of the 'gassing' and 'leaking' holes across the contacting area of a tray. The fraction of 'gassing' holes, f_g may be grouped together or may be uniformly distributed. 'Gassing' holes and 'leaking' holes may be fully segregated, as happens on a tilted tray, for instance. So, the gas flow may become severely maldistributed, longitudinally as well as transversally. Consequently, the separation performance of a tray will be reduced [11]. These phenomena are known to occur on dual flow trays as well and hence should be taken into account upon approach of the dumping region.

3.2. Seal point

The seal point is the gas flow rate, at which the first liquid starts to flow over the outlet weir ($\omega \leq 1$). At this point the two phase layer is expanded to the same level as the height of the outlet weir:

$H_B = H_W$ and as $H_L = \varepsilon_L H_B$;

$H_L = \varepsilon_L H_W$ or in dimensionless form: $\frac{gH_L}{\lambda_h^2} = \frac{\varepsilon_L g H_W}{\lambda_h^2}$

Note however, that at the seal point the dispersion height H_B may not be sharp, but rather diffuse, as a result of the fluctuations in the dispersion. This may present a severe problem, especially upon operation of the tray in the spray regime. For a better description of the seal point under spray regime conditions, a more appropriate relation between (the variability in) dispersion height and liquid flow over an outlet weir will have to be found. Also, the description of the dispersion height in the normal operating range could benefit from such an improved relation. This aspect merits further attention.

3.3. Weeping range

Between the gas flow rate at the seal point and that at the weep point, the tray is weeping and the weep fraction ω varies in the range; $0 < \omega < 1$.

Two dimensionless relationships describe the liquid height at the same time:

$$\frac{gH_L}{\lambda_h^2} = c_1(1 + c_2\sqrt[3]{(\omega\varphi)^2})^3 \tag{3.3.1}$$

$$\frac{gH_L}{\lambda_h^2} = \frac{\varepsilon_L g H_W}{\lambda_h^2} + \frac{(1-\omega) g H_{OW}}{\lambda_h^2} \tag{3.3.2}$$

In principle, the weep fraction can be obtained from these equations, for a given tray geometry and with given flows, by using an iterative procedure.

3.4. At the weep point and beyond (normal operating range)

At the gas flow rate defining the weep point, any leakage of liquid stops and the holes are used exclusively by the gas. This condition can be obtained from the above two relations as well, by recognising that at this point $\omega \to 0$. Hence, in dimensionless form, the criterion is; $(\varepsilon_L g H_W)/\lambda_h^2 + [(1-\omega) g H_{OW}]/\lambda_h^2 = c_1$.

The liquid height is commonly calculated via:

$$H_L = \varepsilon_L H_W + H_{OW} \tag{3.4.1}$$

or in dimensionless form:

$$\frac{gH_L}{\lambda_h^2} = \frac{\varepsilon_L g H_W}{\lambda_h^2} + \frac{g H_{OW}}{\lambda_h^2} \tag{3.4.2}$$

The weir crest contribution will be calculated as: $H_{OW} = (Q_L/L_W)/V_{l,OW}$.

The Francis weir formula is commonly used to calculate the weir crest contribution of the liquid height. This is also done here, although the weir crest equation has not been validated for use in the heterogeneous bubbling flow regime. With clear liquid flowing over a weir: $V_{l,OW} = [gQ_L/L_W]^{1/3}/1.43$. For operation in the spray regime, the characteristic velocity for passage of the 'splashing' liquid drops over the weir has yet to be worked out. When that has been achieved, it can be combined with the above formulation of the weir crest contribution.

An additional remark is in order with respect to the complete stopping of weepage, at and beyond the weep point. The criterion just given above is based on an overall pressure balance, which is equilibrated in a time- and position-averaged sense. However, because of the chaotic fluctuations of the liquid movements in the dispersion, some leakage persists (but at declining rates) at gas rates above the weep point. Note, that these are mainly due to downward components in the velocity distribution of the movements in the overlying dispersion. The upward moving part of the fluctuation spectrum is missing, because these move upward and away. The liquid leakage will become zero only a little above the weep point criterion specified above.

3.5. Linearization of the weeping range liquid height model

As long as the hole flow parameter, $\omega\varphi$ satisfies $\omega\varphi \lesssim 2$, the exponential terms in Eq. (3.3.1) can be simplified and approximated by:

$$\frac{gH_L}{\lambda_h^2} = c_1(1 + c_3\omega\varphi) \tag{3.5.1}$$

Admittingly, this puts a restriction on the range of applicability of this equation.

Combination of Eqs. (3.4.1) and (3.5.1) results in a simple relation for the weep fraction:

$$\omega = \frac{\left(\frac{\varepsilon_L g H_W}{\lambda_h^2} + \frac{g H_{OW}}{\lambda_h^2} - c_1\right)}{\left(\frac{g H_{OW}}{\lambda_h^2} + c_1 c_3 \varphi\right)} \tag{3.5.2}$$

This explicit equation is the relation being sought. It shows why weepage has been so difficult to measure experimentally and predict theoretically. The weep fraction depends on the liquid fraction ε_l (which depends on the system, tray type, tray geometry and gas flowrate), on three dimensionless groups of variables (including φ) and on two tray specific constants. All these parameters have to be known or carefully controlled during testing.

Two limiting cases can be recovered: the seal point (at $\omega = 1$) and the weep point (at $\omega = 0$). The dimensionless seal point vapour rate is:

$$\frac{\lambda_{h,sp}^2}{gH_W} = \frac{\varepsilon_L}{c_1(1+c_3\varphi)}$$

and the dimensionless weep point vapour rate:

$$\frac{\lambda_{h,wp}^2}{gH_L} = \frac{1}{c_1}$$

which essentially is the same criterion as proposed by Lockett and Banik [14] and Banik [15]. The importance of the outlet weir can be emphasised by writing:

$$\frac{\lambda_{h,wp}^2}{g(\varepsilon_L H_W + H_{OW})} = \frac{1}{c_1}$$

Then, the turndown in gas flow rate from weep point to seal point can be written as:

$$\frac{\lambda_{h,sp}}{\lambda_{h,wp}} = \frac{1}{\sqrt{1+c_3\varphi}\sqrt{1+\dfrac{H_{OW}}{\varepsilon_L H_W}}}$$

Note, that for very large liquid flow rates (when the flow parameter, $\varphi \to \infty$) the seal point gas flow rate is expected to go to zero: a tray should no longer possess a minimum gas flow rate. For very small liquid rates (when $\varphi \to 0$ and $H_{OW} \to 0$), the weep and seal point become identical. Obviously, before this limit is reached, the transition from bubbling regime to spray regime will be encountered, which thus puts a limit on the applicability of these equations. This regime transition is estimated to occur in the range of flow parameters range: $\approx 0.03 < \varphi < \approx 0.05$. This gives an approximate lower limit for the range of flow parameter values in which the equations may be used.

4. Validating the model and retrieving the parameters

The key to the model presented here is the new liquid height equation. This equation needs to be validated. Only two sets of experimental data were found to admit such an analysis; viz. (1) data obtained by Banik [15] in his PhD thesis at UMIST (UK), and (2) some data obtained in an air/water tray simulator at Shell Research and Technology Centre, Amsterdam (SRTCA).

The experimental set up used by Banik for collecting of his weep rate data was a rectangular column of 1.22 m length × 0.63 m width, containing four sieve or valve trays and a chimney tray for collecting the leaking liquid. Five different sieve tray layouts and one Glitsch V-1 valve tray layout were tested. The outlet weir heights were either 25, 51 or 76 mm high. The test systems used were air/water and air/Isopar M. For each layout the effect of gas flow rate, liquid flow rate and weir height were studied. All further details of the test unit can be found in Refs. [14,15].

The data analysis requires that the gas flow rate, liquid flow rate, weep rate and liquid height should be available. The data on gas flow rate, liquid flow rate and weep rate were taken directly from Banik's thesis [15]. Not all his weep rate data were used however. For a meaningful test of the liquid height correlation, only those runs were selected for which leakage was more than 10% of the liquid flow rate; $\omega > 0.1$. Banik did not allow his trays to operate at or below the seal point, so all selected data fell in the weeping range; $0.1 < \omega < 1.0$. The liquid height was derived by averaging the seven static liquid height measurements, longitudinally positioned in the liquid flow path from tray inlet to outlet. Two points nearest to the tray inlet and two nearest to the outlet were used to obtain a liquid height ratio at inlet and outlet. Subsequently, this inlet/outlet ratio was used to remove those test data for which this ratio deviated by more than 30% from unity. In this way, longitudinally non-uniform flow patterns were eliminated from the database. As indicated above, there are a number of other phenomena that may complicate the analysis. Therefore the data have been scrutinised and freed from those data, when they were found to be affected. Additionally, for the valve tray data, the gas flow rate was required to be high enough for the valves to be in a floating or fully opened position. After screening, a total of 250 datapoints remained for analysis (213 for the five sieve trays and 37 for the valve tray).

The SRTCA tray simulator was a rectangular column also, with a contacting area of 0.60 m length × 0.37 m width. Two tray layouts were tested. Below the test tray, a chimney type draw off tray collected the total amount of weepage. The first tray layout was a sieve tray with sharp edged holes facing the incoming gas. The second was a valve tray with Metawa/Shell snap in valves. The weir had a fixed height of 0.10 m which extends the range covered Lockett and Banik. There are 42 datapoints, all on the air/water test system.

The data gathered on the SRTCA tray simulator supplement and extend Banik's data. The selection criteria applied to these data were the same as for his data. Data acquisition was executed in a similar way. The liquid height was found by various methods; by a time-averaged static pressure measurement on the tray floor, by integration of the dispersion density profile obtained by gamma ray attenuation measurements or simply by observing the liquid height accumulating at the inlet and outlet edges of the tray. In the lower operating range, described here, these methods produce values which are in good agreement.

Figs. 4 and 5 give examples of plots of dimensionless liquid height versus hole flow parameter. The first graph is for Banik's sieve tray layout SA and the other for Banik's Glitsch V-1 valve tray. The flow parameter in these plots is based on the amount of liquid actually leaking through the perforations; $\varphi_h = \omega\varphi$. The graphs show the available data points along with a best fitting linear regression line. For the air/water system in Fig. 4, the effect of linearization of the original exponential expression (Eq. (3.1.2.6)) is shown. The short dashed line represents a linear regression line and the fully drawn line labelled 'Expon.' represents the original exponential expression with the same coefficient c_1. The coefficient c_2 was chosen in such way that the same correlation

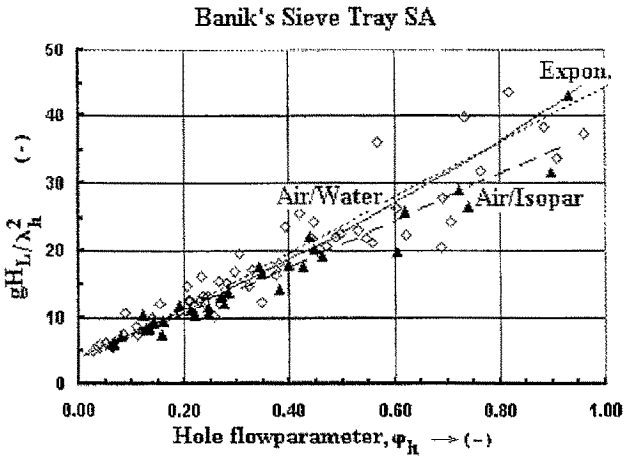

Fig. 4. Banik's data. Sieve tray SA.

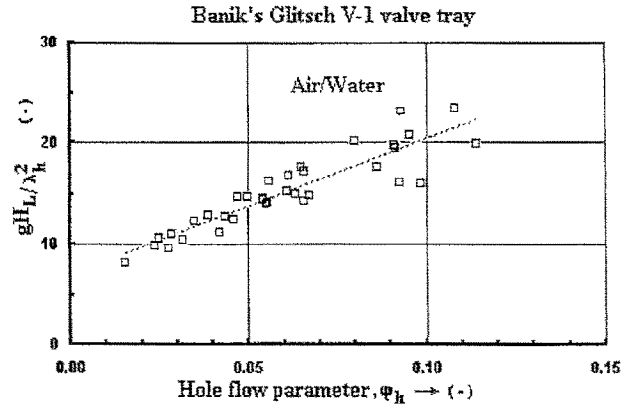

Fig. 5. Banik's data. Glitsch V-1 valve tray.

coefficient resulted. Considering the spread in the data, it will be clear from the comparison of these two lines that the loss in accuracy by linearization is limited in the range of flow parameters considered.

Several observations can be made from graphs 4 and 5.

(1) The simple approximating equation worked reasonably well for both sieve and valve trays. Considering the assumptions made in the derivation of equation, these results are encouraging.

(2) The two different test systems used by Banik gave similar results. So much so, that a regression analysis showed that the overlap was sufficient to make them essentially indistinguishable. This meant that differences in liquid viscosity and surface tension of these two systems do not have a large effect.

(3) The liquid flow rate, incorporated in the hole flow parameter affects the liquid height significantly. The competition of the gas and the liquid flow for the free hole area accounts for the increase in liquid height. At higher flow parameters, this contribution can be large; much larger than the contribution of the gas hole pressure drop (given by the ordinate intercept).

(4) The valve tray figure is important. It shows that the increased gas pressure drop coefficient, in comparison to the sieve trays, increased the liquid hold up. This was reflected by the increase in intercept and the slope, as expected. This confirms the pressure balance approach of the model.

(5) Comparison of the sieve tray and valve tray plots showed, that at the same liquid height a valve tray weeps less than a sieve tray, and that at the same flow parameter a valve tray has a higher liquid hold up.

The numerical results of the analysis for all individual tray layouts are given in Table 1. These results strengthen the above observations. A few others can be added.

The ordinate intercept gives the value of the constant c_1. For all sieve tray layouts, the c_1-coefficients are similar, except for Banik's layout SC. The SRTCA sieve tray data give support to Banik's sieve tray data and extend the range of application to a higher weir height. The hole diameter and the amount of free area appear to have no observable effect. Banik's sieve tray SC combined a long flow path length ($L_{fp}=0.98$ m) with the highest free area. This combination caused this tray to weep preferentially at the inlet of the tray (next to the inlet downcomer) and produced a substantial 'hydraulic gradient'. In order to fulfil the hydraulic gradient selection criterion, a large part of these datapoints have been discarded. However, this procedure may not have been selective enough in identifying test conditions, with the most uniform weeping pattern.

All c_1-values are about 3- to 5-times the dry pressure drop coefficient, for both tray types. This increase is explained by the large temporal fluctuations in gas flow rate and hole pressure drop as caused by the bubble formation process. The consequence of this is also, that a change in gas flow pattern at the perforations to a more steady regime (as with the formation of gas jets) will result in a reduction of the pressure drop of the 'gassing' holes and increased weeping from the 'leaking' holes. As a state of lower energy dissipation will be attained, this type of operation will stabilise itself. The low c_1-value for Banik's sieve tray layout SC indicates, that such

Table 1
Best fitting constants for the dumping range liquid height equation

Data source	Tray	Layout identifier	D_h (mm)	Free area (%)	$\xi_g/2$ (c_{dry})	c_1	c_2	c_3
SRTCA data	Sieve	–	12.0	13.7	1.10	2.9	1.76	20.0
Banik's thesis	Sieve	SA	12.7	10.2	0.83	3.8	1.76	20.0
Banik's thesis	Sieve	SB	12.7	14.1	0.84	3.7	1.76	20.0
Banik's thesis	Sieve	SC	12.7	19.4	0.67	1.9	1.76	20.0
Banik's thesis	Sieve	SD	6.35	10.2	0.73	3.0	1.76	20.0
Banik's thesis	Sieve	SE	3.17	9.7	0.62	3.5	1.76	20.0
Banik's thesis	Valve	Glitsch V-1	38.1	23.8	2.5	7.0	2.24	33.0
SRTCA data	Valve	Metawa	40.0	15.7	2.3	12.8	2.14	30.0

a change in flow regime might indeed have been triggered. This distinctive change in tray behaviour may have been spotted already during the early stages of the sieve tray development by d'Ancona Hunt et al. [18] and McAllister et al. [19].

The difference in the c_1-values for the two different types of valve trays cannot be accounted for only by the difference in the dry pressure drop coefficients for fully opened valves. As most of the selected data were for valves operating in their 'floating' state (in transition between closed and fully open), valve weight controls the hole gas pressure drop. The Metawa/Shell snap-in valves were 31 g/piece and the Glitsch V-1 valves 26 g/piece. The heavier valve indeed has the higher c_1-value and at the same liquid height the lowest leakage. This conclusion finds confirmation in tests done by Norman and Grocott [20] on valves with three different weights. They reported a consistent and large decrease in leakage by increasing the valve weight.

From the slope of the curves, the c_3-values are calculated and also the c_2-values are derived. These c_2-values are of the order of unity, as expected for the ratio of the liquid to gas flow resistance coefficients. The values for the valve trays indicate, that on these trays the ratio was somewhat larger in comparison to sieve trays. This was not unexpected considering the action of the valves, whose purpose it is to enhance the resistance to liquid flow more than the resistance to gas flow.

Overall, the liquid height equation gives a satisfactory description of the data and also makes them understandable. Remember, that the available data allowed the relation to be tested with a somewhat limited precision, however.

5. Application to other data

In the open literature, the amount of data available on sieve tray weep points is fairly large. The seal point has gained much less attention. Data on weep rates, apart from the information already used, is meagre to say the least.

Sieve tray weep point data have been retrieved mainly from Refs. [2,4,14,18,21–24]. In all, 177 values for the weep point hole load factor were secured (along with 10 redefined weep points taken from Banik [15]). Included in this data set are values obtained for various systems, a range of weir heights, free area's, hole sizes and liquid loads. The weep point has been identified by various means: visually, by observation of amount of holes leaking; graphically by locating a break (kink) in the pressure drop curve and by measuring the amount of weepage directly. Taking all these data at face value and simple averaging them produced for the hole load factor the value: $\lambda_{h,wp} = 0.35 \pm 0.07$ m/s. Irrespective of the means of identification, the weep points were identified fairly consistently by different authors. As a first estimate of the position of the weep point hole load factor, this constant value is good enough. However, a distinctive underlying pattern of effects could be discerned. An analysis of the parameters involved revealed that liquid height, H_L and hole free area were the only parameters having any effect. The best nonlinear regression was obtained with: $\lambda_{h,wp} = 0.33 \pm 0.05[(H_L/0.05)(0.10/f_h)]^{0.20}$. Here liquid height and free area have been compared to reference values of 50 mm liquid height and 10% free area. Another way of summarising the weep point data was by defining a hole Froude number as $Fr_{h,wp} = \lambda_{h,wp}/\sqrt{gH_L}$; the best fitting value was found to be $Fr_{h,wp} = 0.59 \pm 0.13$.

According to the pressure balance model, the expected value for the weep point Froude number is: $Fr_{h,wp} = \sqrt{\lambda^2_{h,wp}/gH_L} = \sqrt{1/c_1}$. With $c_1 = 3$–4 (see Table 1), it was calculated as $Fr_{h,wp} = 0.50$–0.58, which agrees within the uncertainty of the experimental Froude number values. It was recognised, that for most tests in the data set the liquid height ranged within certain limits, only: $0.025 \leq H_L$ (m) ≤ 0.065. This meant also, that the weep point hole load factor varied within limits: $0.27 \leq \lambda_{h,wp}$ (m/s) ≤ 0.44. Hence, the weep point hole load factor could be seen to be constant with an average value of $\lambda_{h,wp} = 0.36 \pm 0.09$ m/s. This latter value is in good agreement with the average value obtained for the whole experimental data set. The free area effect could be explained by the contribution of the weir height in association with the liquid fraction in the dispersion to the total liquid height on the tray. The liquid fraction in the dispersion, ε_l depends primarily on the load factor based on the contacting area. The empirical equation $\varepsilon_l = 0.95\exp(-17\lambda_h f_h)$ gave a reasonable description of Banik's sieve tray data. Using this relation to produce some calculated results (for the range of weir heights and free areas used in the data set) and subsequent regression, it could be shown that $\lambda_{h,wp} \propto f_h^{-0.20}$. This came close enough to the value for the exponent found before, to verify the origin of the free area effect. Indirectly, this confirmed that variations in the liquid fraction in the dispersion affect the weep point. This is important in comparisons of results for different test systems, which may have different surface properties (foaming tendencies). Keeping this in mind and remembering that the data set includes various aqueous and organic systems, the variability in the weep point data gets a new meaning.

Lockett and Banik [14] reported the value $Fr_{h,wp} = 0.67$. It is worth noting that their weep point was defined at effectively 0% weep fraction (as a result of extrapolation to a weep rate of 0 $m^3/(m^2\ s)$). By redefining their weep point data at 10% weepage and recalculating their Fr-values, a value of $Fr_{h,wp} = 0.40$ was obtained. This shows two things. Firstly, that at low percentages of weeping, the definition of the weep point is of importance. Secondly, that their data are compatible with the proposed Fr-value, which apparently allows a few percent of weepage. This was expected, because higher hole velocities are needed to remove the last percent of weepage. This small but persistent leakage in the tail end of the weep fraction curve is caused by the high velocity part of the spectrum of stochastic liquid movements in the dispersion.

All this leads to the conclusion, that the weep point criterion, derived from the pressure balance model ($Fr_{h,wp} = 0.54 \pm 0.04$) is in agreement with available experimental data.

Sieve tray seal point (dump point) data were derived from Refs. [2,5,21,25]. In all, 42 values for the seal point hole load factor were used, including the SRTCA seal point data. The seal point gas flow rates were identified either by a distinct break (fall off) in the tray pressure drop curve [21,25] or by finding the 100% weepage point from weep rate measurements [2].

The early efforts of Prince and Chan [5] had established already, that the seal point depended mainly on flow parameter, φ and weir height. The pressure balance model calculates the seal point written as a Froude number as $Fr_{h,sp} = \sqrt{\lambda_{h,sp}^2/gH_w} = \sqrt{\varepsilon_l/[c_1(1+c_3\cdot\varphi)]}$. Again, using $c_1 = 3$–4, $c_3 = 20$ and the empirical liquid fraction correlation $\varepsilon_l = 0.95\exp(-17\lambda_{h,sp}f_h)$ the Froude number was calculated as $Fr_{h,sp} = 0.52\sqrt{\exp[-17\lambda_{h,sp}f_h]/[1+20\varphi]}$. (The terms under the square root can be seen as correction factors for free area and flow parameter respectively). The calculated values were compared to experimental values. This comparison yielded as a ratio of Froude numbers (calculated $Fr_{h,sp}$/experimental $Fr_{h,sp}$) $= 0.96 \pm 0.25$ (see the parity plot in Fig. 6). Again, this was an encouraging result. Overall, there was a larger variability in the correlation of the seal point data than in the weep point data, however. The observed scatter in the data is probably caused by the empirical liquid fraction correlation, which neglects (changes in) the actual surface properties of the test system. Experience has shown that for the system air/tap water the surface properties and hence the coalescence behaviour can vary visibly. The additional parallel indications, that there were small effects in the data of: (1) the test system (being an aqueous system or an organic system) and (2) the weir height (by changes in the shape of the vertical liquid density profile), also pointed to limitations of the liquid fraction correlation.

This leads to the conclusion, that the seal point criterion, derived from the pressure balance model, is in reasonable agreement with separately available experimental seal point data and that observed discrepancies can readily be understood by shortcomings in the correlation of the liquid fraction in the dispersion.

The turndown in the weeping range was not evaluated separately, because the only check available were the data points of Brambilla et al. [2], which had already been used in the weep- and seal point evaluations. So, no additional insight would be gained. However, it might be noted, that their seal points were located far below their weep points: $0.33 \le \lambda_{h,sp}/\lambda_{h,wp} \le 0.63$.

Another way to visualise the switch in tray behaviour from normal operation to weeping and to dumping when lowering the gas rate, is by calculating the expected weep fraction and liquid heights and presenting the results graphically. For purposes of comparison and elucidation, the same sieve tray layout and operating conditions were chosen as used by Lockett and Banik in their example (figure 23 in Ref. [14]). The lines in Figs. 7 and 8 present the results calculated from the solution of the two liquid height equations, while the points represent the data, taken from Ref. [15].

This calculation demonstrates a number of points:

- The proposed method can reproduce the measured liquid height curve.
- The liquid height in the weeping range is nearly constant. This height falls off below the seal point.

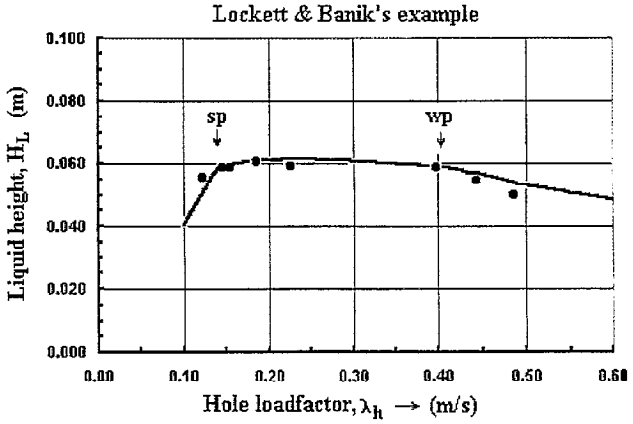

Fig. 7. Example calculation of liquid height.

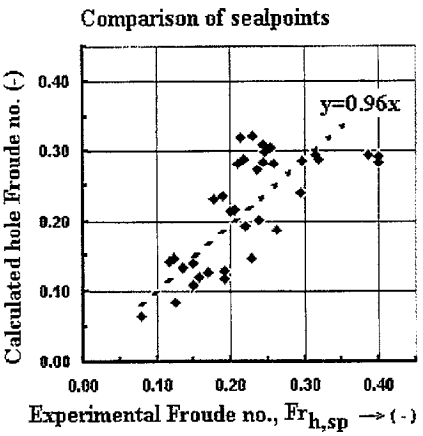

Fig. 6. Seal point comparison.

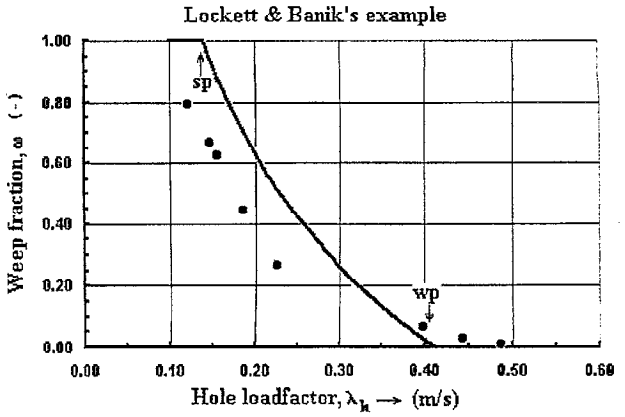

Fig. 8. Example calculation of weep fraction.

– The calculated dependence of weep fraction agrees approximately with the data.
– The non-uniform flow patterns observed [14,15] do not invalidate the calculation method.

6. Effect of weeping on tray efficiency

Operating a tray below its weep point has long been thought to have a detrimental effect on its the tray efficiency. Contrary to this expectation, experimental studies [2,4] have shown, that tray efficiency remained good (at about the same level as during normal operation) down to gas velocities at which most of the liquid is leaking away. In particular, Brambilla et al. [2] showed that their water evaporation efficiencies for a sieve tray remained good even down to the seal point (at 100% weeping). Also, the distillation tray efficiencies reported by Hellums et al. [25] showed this constancy in efficiency down to the seal point (i.e., their fall off point in both pressure drop and efficiency). That the efficiency in the weeping range is constant can be explained by several counteracting effects: (1) The efficiency is reduced by the change from cross flow to countercurrent flow, as shown for uniform weepage by Lockett et al. [3] and Kageyama [26]. The efficiency is also reduced by non-uniform flow patterns [14,15,27]. (2) The leaking liquid offers additional interfacial area for mass transfer. This contribution is difficult to quantify. (3) The liquid height in the weeping range is fairly constant according to the calculations presented here. (4) As the gas flow rate goes down in the weeping range so does the mass transfer coefficient.

This means that the weep point should not be considered the lower operating limit of a tray. It is at most an early warning of what will happen near the real minimum operating limit, the seal point.

This can be demonstrated by two examples. In Fig. 9, efficiency curves are plotted of an 8% free area sieve tray and an 19% free area Glitsch V-1 valve tray based on published F.R.I. data [21,28]. Both data sets were from F.R.I.'s 1.2 m diameter distillation column, operating with a cyclohexane/*n*-heptane test mixture at 1.65 bar. Both had a weir with a height of 51 mm and a length of 0.9 m. The efficiency data are replotted against the hole load factor. The weep point and the weep fractions calculated with the method given here, are also plotted. It is seen that the efficiency of the valve tray only goes down when practically all liquid is weeping through the valves. The lowest point for the sieve tray was still above the seal point (as could be seen from the tray pressure drop curve also). The calculated weep point agreed nicely with the reported experimental weep point [21].

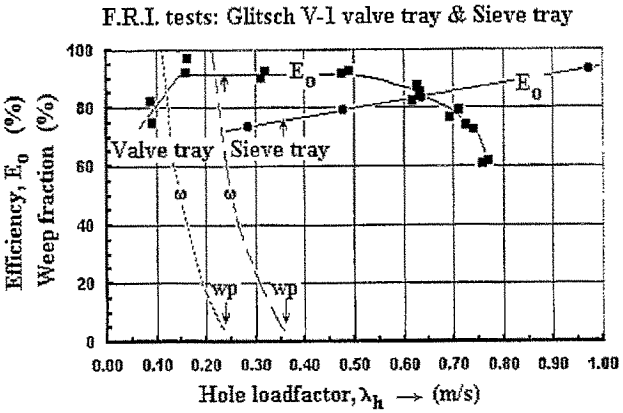

Fig. 9. Efficiency and weeping compared for a sieve and a valve tray.

Modelling the liquid height along with the weep fraction has been the object of this paper. The model has a non-uniform hydraulic two region approach at its base. For simplicity, it was assumed that the 'gassing' regions and the 'leaking' regions were uniformly distributed across the contacting area. This would lead to the expectation of a uniform flow distribution, when observing the flow behaviour at a sufficiently large length scale (larger than 0.05–0.1 m). However, there is no compelling reason why this should be the case (other than, that a simple model could be constructed in this way). Maldistribution of the flows of gas through and liquid across and through the tray may develop, as they are not excluded by the proposed model (they are even an integral part of it). So, the type and degree of maldistribution in the gas and liquid flows and the effect this has on efficiency remains to be studied. As long as this problem stays around, small scale experimental efficiencies can only be extrapolated to a larger scale with limited accuracy. Some useful work can still be done.

On the basis of the understanding gained by this study, it should be possible to make more optimal use of the (potential) turndown capabilities of existing absorption and distillation columns, equipped with sieve or valve trays, and to tailor new tray designs better to the flexibility required of absorption and distillation columns.

7. Conclusions

A new method of calculating the minimum gas flow rates of sieve and valve trays, operating in the 'churn turbulent, bubbling' flow regime, has been proposed and validated. The method relies on the simultaneous solution of two different liquid height equations, the first being the common equation for normal tray operation and the second a new equation, describing the liquid height on a tray without downcomers (a 'dual flow' tray). It has been shown, that the position of the lower operating range (in terms of minimum gas flow rates) can be calculated by this method. The connection between weeping and tray efficiency was revisited. It was argued that use of the weep point as a lower limit can be relaxed and be replaced by a point approaching the seal point. With the understanding gained, it will be possible to make better use of the flexibility of sieve and valve trays.

8. Nomenclature

Parameter	Description	Units
A_h	hole area	m^2
c_1; c_2; c_3	flow resistance coefficients, for two phase flow	–
c_{dry}	flow resistance coefficient, gas flow only (= dry)	–
D_h	orifice or hole diameter	m
E_o	Overall (Fenske) efficiency	–
f_g	fraction of holes in the 'gassing' state	–
f_h	hole area as fraction of contacting area (= free area)	–
f_l	fraction of holes in the 'leaking' state	–
F_h	F-factor based on hole area $[= V_{gh}\sqrt{\rho_g}]$	$(m/s)(kg/m^3)^{1/2}$
Fr_h	Froude number, based on hole load factor $[= \lambda_h/\sqrt{gH_L}]$	–
g	gravitational acceleration	m/s^2
$h_{b,g}$	height of two phase layer on the 'gassing' part of a tray	m
$h_{l,g}$	liquid height on the 'gassing' part of a tray	m
$h_{l,l}$	liquid height on the 'leaking' part of a tray	m
H_B	height of two phase layer (= bed height)	m
H_L	equivalent clear liquid height in the two phase layer on the entire tray	m
H_{OW}	liquid height over outlet weir	m
H_W	outlet weir height	m
L_{fp}	length of flow path	m
L_w	overflow length of outlet weir	m
P_1 to P_6	pressure	N/m^2
Q_g	volumetric gas flow rate	m^3/s
Q_L	volumetric liquid flow rate	m^3/s
V_{gh}	gas velocity in the holes $(= Q_g/A_h)$	m/s
V_{lh}	liquid velocity in the holes $(= Q_L/A_h)$	m/s
$V_{l,OW}$	horizontal liquid flow velocity, over weir	m/s
Δh_l	difference in liquid height	m
ΔP	difference in pressure (= pressure drop)	N/m^2
ε_L	liquid volume fraction in two phase layer	–
λ_h	hole load factor (= hole capacity factor) $[= F_h/\sqrt{\rho_l - \rho_g}]$	m/s
$\lambda_{h,sp}$	hole load factor (= hole capacity factor) $[= F_h/\sqrt{\rho_l - \rho_g}]$ at seal point	m/s
$\lambda_{h,wp}$	hole load factor (= hole capacity factor) $[= F_h/\sqrt{\rho_l - \rho_g}]$ at seal point at weep point	m/s
ρ_g	gas density	kg/m^3
ρ_l	liquid density	kg/m^3
φ_h	hole flow parameter (= $\omega\varphi$)	–
φ	flow parameter $[= (Q_L/Q_g)\sqrt{\rho_l/\rho_g}]$	–
ω	weep fraction (fraction of total liquid flow leaking away through perforations)	–
ξ_g; ξ_l	pressure drop coefficient for flow of gas or liquid, respectively	–
$\xi_{g,g}$	pressure drop coefficient for gas flowing through holes in the 'gassing' state	–

Acknowledgements

The author is grateful to Shell International Oil Products for their support and allowance to make use of data generated during his employment at Shell Research and Technology Centre, Amsterdam. He wishes to recall the initial ideas of R. (Richard) C. Darton on this subject, as they guided him in finding his own direction. The contribution of G. (Gert) Konijn was essential in obtaining the SRTCA test data. Discussions with J. (Hans) A. Wesselingh have been most helpful to the author in putting his thoughts on paper in a clear and structured manner.

References

[1] J.A. Wesselingh, Non-equilibrium modelling of distillation, Distillation and Absorption '97, I. Chem. E. Symposium Series No. 142, Maastricht, September 1997, pp. 1–21.
[2] A. Brambilla, E. Gianolo, G.F. Nencetti, Fluodynamic behaviour and efficiency of sieve trays at low gas rates, I. Chem. E. Symposium Series No. 56, 1979, pp. 3.2/1–3.2/20.
[3] M.J. Lockett, M.A. Rahman, H.A. Dhulesia, Prediction of the effect of weeping on distillation tray efficiency, AIChE J. 30 (3) (1984) 423–431.
[4] H. Mustafa, E. Békássy-Molnár, Influence of weeping on mass transfer rate of different plates, Trans. I. Chem. E. 73 (1995) 392–397 Part A.
[5] R.G.H. Prince, B.K.C. Chan, The seal point of perforated distillation plates, Trans. Inst. Chem. Engineers 43 (1965) T49–T55.
[6] M.W. Biddulph, D.J. Stephens, Oscillating behaviour on distillation trays, AIChE J. 20 (1) (1974) 60–67.
[7] M.W. Biddulph, Oscillating behaviour on distillation trays—II, AIChE J. 21 (1) (1975) 41–49.
[8] J.O. Hinze, Oscillations of a gas/liquid mixture on a sieve plate, Symp. on Two Phase Flow, University of Exeter, UK, 1965, p. F101.
[9] E.F. Wijn, Pulsations of the two phase layer on trays, I. Chem. E. Symposium Series No. 73, 1982, pp. D79–D101.
[10] H.Z. Kister, K.F. Larson, P.E. Madsen, Vapor crossflow channelling on sieve trays: fact or myth?, Chem. Eng. Prog. 88 (11) (1992) 86–93.

[11] M.J. Lockett, On tilted trays, Chem. Eng. Res. Des., Trans. I. Chem. E. 69 (1991) 99–107.
[12] W.J. Beek, Oscillations and vortices in a batch of liquid sustained by a gas flow, Symp. on Two Phase Flow, University of Exeter, UK, 1965, pp. F401–F406.
[13] H.F. Haug, Stability of sieve trays with high overflow weirs, Chem. Eng. Sci. 31 (1976) 295–307.
[14] M.J. Lockett, S. Banik, Weeping from sieve trays, Ind. Eng. Chem. Process. Des. Dev. 25 (1986) 561–569.
[15] S. Banik, Weeping from distillation trays, PhD Thesis, University of Manchester Institute of Science and Technology, Manchester, UK, October 1982.
[16] M. Prado, The bubble-to-spray transition on sieve trays: mechanisms of the phase inversion, PhD Thesis, Univ. of Texas, Austin, TX, USA, 1986.
[17] A.E. Wraith, Two stage bubble growth at a submerged plate orifice, Chem. Eng. Sci. 26 (1) (1971) 1659–1671.
[18] C. d'Ancona Hunt, D.N. Hanson, C.R. Wilke, Capacity factors in the performance of perforated-plate columns, AIChE J. 1 (4) (1955) 441–451.
[19] R.A. McAllister, P.H. McGinnis Jr., C.A. Planck, Perforated-plate performance, Chem. Eng. Sci. 9 (1958) 25–35.
[20] W.S. Norman, G.J. Grocott, Factors affecting the performance of valve plates, Trans. Inst. Chem. Engineers 39 (1961) 305–312.
[21] M. Sakata, T. Yanagi, Performance of a commercial scale sieve tray, I. Chem. E. Symposium Series No. 56, 1979, pp. 3.2/21–3.2/33.
[22] R.G.H. Prince, Characteristics and design of perforated plate columns, International Symp. on Distillation, 1960, pp. 177–184.
[23] F.D. Mayfield, W.L. Church, A.C. Green, D.C. Lee, R.W. Rasmussen, Perforated-plate distillation columns, Ind. Eng. Chem. 44 (9) (1952) 2238–2249.
[24] D.S. Arnold, C.A. Planck, E.M. Schoenborn, Performance of perforated-plate distillation columns, Chem. Eng. Prog. 48 (12) (1952) 633–642.
[25] J.D. Hellums, C.J. Braulick, C.D. Lyda, M.v. Winkle, Perforated plate efficiency—effect of design and operating variables, AIChE J. 4 (4) (1958) 465–471.
[26] O. Kageyama, Plate efficiency in distillation towers with weeping and entrainment, I. Chem. E. Symp. Ser. No. 32, pp. 2–72.
[27] J.F. Billingham, S. Banik, M.J. Lockett, The effect of inlet weeping on distillation tray efficiency, Trans. I. Chem. E. 73 (1995) 385–391 Part A.
[28] Glitsch, Glitsch Ballast Trays A-1, V-1, V-0, Experimental Test Data, Combined Bulletins No. 159/160 (Revised), June 1983.